DOI: 10.1002/chem.200500879

Vibronic Coupling in Organic Semiconductors: The Case of Fused Polycyclic Benzene–Thiophene Structures

Veaceslav Coropceanu,*[a] Ohyun Kwon,[a, e] Brigitte Wex,[b] Bilal R. Kaafarani,[c] Nadine E. Gruhn,[d] Jason C. Durivage,[d] Douglas C. Neckers,[b] and Jean-Luc Brédas*[a]

Abstract: The nature of vibronic coupling in fused polycyclic benzene–thiophene structures has been studied using an approach that combines high-resolution gas-phase photoelectron spectroscopy measurements with first-principles quantum-mechanical calculations. The results indicate that in general the electron–vibrational coupling is stronger than the hole–vibrational coupling. In acenedithiophenes, the main contributions to the hole–vibrational coupling arise from medium- and high-frequency vibrations. In thienobisbenzothiophenes, however, the interaction of holes with low-frequency vibrations becomes significant and is larger than the corresponding electron–vibrational interaction. This finding is in striking contrast with the characteristic pattern in oligoacenes and acenedithiophenes in which the low-frequency vibrations contribute substantially only to the electron–vibrational coupling. The impact of isomerism has been studied as well.

Keywords: electron transport · electronic structure · heterocycles · photoelectron spectroscopy

Introduction

Oligoacene-based materials represent the most studied[1–6] and promising class of π-conjugated organic semiconductors used as active elements in new generations of plastic (opto)-electronic devices. Pentacene, the major representative of this group, shows a hole mobility of up to 35 $cm^2V^{-1}s^{-1}$ at room temperature[7] and has become the benchmark for p-type organic semiconductors. However, shortcomings, such as poor solubility, limited stability, and unfavorable herringbone packing in the solid state, significantly weaken the commercial viability of pentacene-based devices.

Many attempts have been made to improve on the properties of pentacene by substitution or functionalization.[8–10] Katz and co-workers[11,12] have shown, for instance, that anthradithiophene (ADT) displays improved solubility and stability toward oxidation and exhibits a mobility of 0.15 $cm^2V^{-1}s^{-1}$ that approaches that of amorphous silicon. Anthony et al. have recently demonstrated[6] that, as in the case of pentacene, directed functionalization of the central ring of ADT further increases the solubility and tunes the solid-state ordering in favor of π stacking. More recently, some of us[13,14] reported two thienobisbenzothiophene (TBBT) isomers (see Figure 1), in which, in comparison to ADT, the central benzene ring is also replaced with a thiophene ring. The X-ray analysis[14] of the *anti*-TBBT isomer reveals a favorable molecular overlap along the crystal *c* axis, which suggests that TBBT and their derivatives might be promising materials for applications in organic electronics. The synthesis and characterization of several other acenedithiophenes have been recently reported in the literature.[15,16]

[a] Dr. V. Coropceanu, Dr. O. Kwon, Prof. J.-L. Brédas
School of Chemistry and Biochemistry
Georgia Institute of Technology, Atlanta
Georgia 30332–0400 (USA)
Fax: (+1) 404-894-7452
E-mail: veaceslav.coropceanu@chemistry.gatech.edu
jean-luc.bredas@chemistry.gatech.edu

[b] Dr. B. Wex, Prof. D. C. Neckers
Center for Photochemical Sciences
Bowling Green State University, Bowling Green
Ohio 43403 (USA)

[c] Dr. B. R. Kaafarani
Department of Chemistry, American University of Beirut
Beirut (Lebanon)

[d] Dr. N. E. Gruhn, J. C. Durivage
Department of Chemistry, The University of Arizona
Tucson, Arizona 85721–0041 (USA)

[e] Dr. O. Kwon
Present address: Samsung Advanced Institute of Technology
San 14-1, Nongseo-ri, Giheung-eup, Yongin-si
Gyeonggi-do (Korea)

Supporting information for this article is available on the WWW under http://www.chemeurj.org/ or from the author.

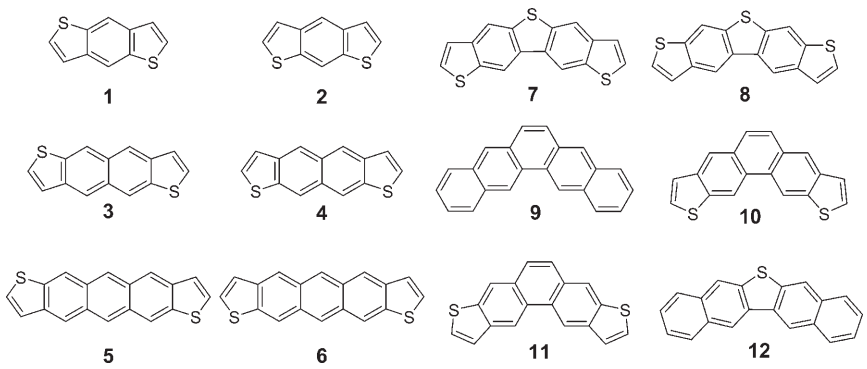

Figure 1. Molecular structures of the compounds investigated in this work: benzo[1,2-*b*:4,5-*b*′]dithiophene (**1**), benzo[1,2-*b*:5,4-*b*′]dithiophene (**2**), naphtho[2,3-*b*:6,7-*b*′]dithiophene (**3**), naphtho[2,3-*b*:7,6-*b*′]dithiophene (**4**), anthra[2,3-*b*:7,8-*b*′]dithiophene (**5**), anthra[2,3-*b*:8,7-*b*′]dithiophene (**6**), thieno[2,3-*f*:5,4-*f*′]bis[1]benzothiophene (**7**), thieno[3,2-*f*:4,5-*f*′]bis[1]benzothiophene (**8**), pentaphene (**9**), phenanthro[3,2-*b*:6,7-*b*′]dithiophene (**10**), phenanthro[2,3-*b*:7,6-*b*′]dithiophene (**11**), dinaphtho[2,3-*b*:2′,3′-*d*]thiophene (**12**).

The efficiency of charge transport, and ultimately the device performance, is controlled by electron–electron and electron–vibration interactions. We have shown recently[17] that the vibronic interactions in ADT are very similar to those in pentacene. Here, we report the hole– and electron–vibrational couplings in a series of fused benzene–thiophene compounds including benzodithiophene (BDT), naphthodithiophene (NDT) and anthradithiophene, see Figure 1. We also investigated the effect on the electronic states and structural reorganization processes produced by modification of the central ring when going from ADT to TBBT. In addition, the possibility of obtaining isomer-pure BDT and TBBT compounds has allowed us to characterize the systems as a function of their isomer constitution. As in our recent work,[17–21] we have used here an approach that combines first-principles quantum-mechanical calculations with high-resolution gas-phase photoelectron spectroscopy measurements. For the sake of completeness and better understanding of the theoretical results, several related systems, such as pentaphene (**9**), phenanthrodithiophene (**10**, **11**), and dinaphthothiophene (**12**) (see Figure 1), are also discussed.

Experimental Section

The BDT (**1** and **2**) and TBBT (**7** and **8**) compounds were synthesized as pure *anti* and *syn* isomers as previously described.[13,14] The gas-phase photoelectron spectra of TBBT and BDT were collected by using the instrument and experimental procedures reported in more detail elsewhere.[22] Both isomers of TBBT sublimed at 190–240 °C and both isomers of BDT sublimed at 55–80 °C. There was no evidence of contaminants present in the gas phase during data collection. The instrument resolution during data collection was better than 35 meV (measured using the full-width-at-half-maximum for the $^2P_{3/2}$ ionization of Ar).

Theoretical methodology: At the microscopic level, the hopping-charge-transport mechanism can be described as a self-exchange electron-transfer process from a charged, relaxed molecule to an adjacent neutral molecule. At high temperature, when the motion of the carriers can be modeled by sequences of uncorrelated hops, the mobility can be given by Equation (1):[23–25]

$$\mu = \frac{ea^2}{k_B T} k_{ET} \quad (1)$$

Here, k_B denotes the Boltzmann constant, T the temperature, e the electronic charge, and a the spacing between the molecules. For a self-exchange reaction the hopping probability per unit time (electron-transfer rate), k_{ET}, is given by Equation (2):[26,27]

$$k_{ET} = A \exp\left[-\frac{\lambda}{4k_B T}\right] \quad (2)$$

Prefactor A depends on the strength of the electronic coupling (i.e., the transfer integral, t): in the case of weak coupling (non-adiabatic ET regime), $A \approx t^2$; in the case of strong coupling (adiabatic ET regime), $A = \nu_n$, in which ν_n is the frequency for nuclear motion along the reaction coordinate. The reorganization energy (λ) results from the molecular geometry modifications that occur when an electron is added to or removed from a molecule (inner reorganization) as well as from the modifications in the surrounding medium due to polarization effects (outer reorganization). It is important to note that due to the weakness of the van der Waals interactions among organic molecules, the separation of the reorganization energy into inter- and intramolecular contributions remains largely valid even in the case of molecular crystals. However, in contrast to electron transfer in solution in which the reorganization energy is usually dominated by outer contribution, in crystals the intramolecular contribution is expected to be of the same magnitude as, or to dominate over the contribution of the surroundings.[28] Here, we focus on the intramolecular vibronic couplings.

Figure 2 represents the potential-energy surfaces of the donor (D) and acceptor (A) related to a intermolecular electron-transfer reaction[2] of

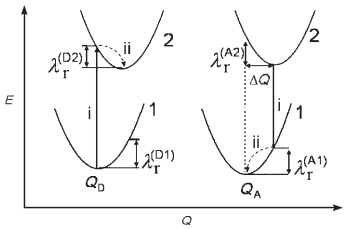

Figure 2. Sketch of the potential-energy surfaces related to electron (hole) transfer, showing the related transitions, the normal mode displacement ΔQ, and the relaxation energies λ_r.

the type $D + A^+ \rightarrow D^+ + A$; the electronic states D1 [A1] and D2 [A2] correspond to the ground state of the neutral and charged (cation or anion) configurations of the donor [acceptor], respectively. As discussed elsewhere in more detail,[2,18] the intramolecular reorganization energy upon electron transfer is given by Equation (3):

$$\lambda_{reorg} = \lambda_r^{(A1)} + \lambda_r^{(D2)} \quad (3)$$

These two energy terms have been computed here directly from the adiabatic potential energy surfaces as shown in Figure 2 (for more details see references 2 and 18). The contribution of each vibrational mode to λ_r has been obtained by expanding the respective potential energies in a power

series of the normal coordinates. In the harmonic approximation, the relaxation energy λ_r is given by Equations (4) and (5).

$$\lambda_r = \sum \lambda_j = \sum \hbar\omega_j S_j \quad (4)$$

$$\lambda_j = \frac{k_j}{2}\Delta Q_j^2 \qquad S_j = \lambda_j/\hbar\omega_j \quad (5)$$

In theses equations the summations run over the vibrational modes, ΔQ_j represents the displacement along normal mode j between the equilibrium positions of the two electronic states of interest, k_j and ω_j are the corresponding force constants and vibrational frequencies, and S_j denotes the Huang–Rhys[26,27] factor (hole– or electron–vibration coupling constant). We note that the Huang–Rhys factors are related to largely used in the literature dimensionless counterpart Δ_i of the displacements ΔQ_j as $S_i = \Delta_i^2/2$. The geometry optimizations of the neutral, cation, and anion species, and the calculations of vibrational normal modes were performed with the Gaussian-98 program[29] at the B3LYP/DFT level using the 6-31G** basis set.

Results and Discussion

Photoelectron spectroscopy: The photoelectron spectra of the BDT and TBBT isomers are shown in Figures 3 and 4, respectively. For the sake of comparison, the previously reported spectra of anthracene,[20] pentacene[20] and ADT[17] are given as well. The first ionizations of both *syn*- and *anti*-BDT isomers have vertical energies of 7.585 ± 0.001 eV and 7.573 ± 0.001 eV, respectively, values close to that of 7.421 ± 0.001 eV for anthracene. The first ionization energies for the *syn* (**7**) and *anti* (**8**) TBBT isomers, 7.36 ± 0.02 and 7.43 ± 0.02 eV, respectively, are larger by about 0.7–0.8 eV than those of ADT[17] (6.699 ± 0.001 eV) and pentacene[20] (6.589 ± 0.001 eV).

As seen from Figure 3, the photoelectron spectra of the BDT isomers are nearly identical. The same must hold true for the ADT isomers; indeed, even though ADT has been obtained as an inseparable mixture of *anti* and *syn* isomers, the sharpness of its photoelectron spectrum (see Figure 4) demonstrates that the cation spectra of the ADT isomers are equivalent. This conclusion is further supported by the electronic-structure calculation; the DFT results indicate that the energy spectrum becomes less dependent on isomer constitution as the size of the system increases. In contrast to the acenedithiophenes, the difference between the photoelectron spectra of the TBBT isomers (see Figure 4) is substantial.

Fused thiophene versus fused benzene—S versus C=C: Previous photoelectron studies[30,31] of several thiophene-containing heterocyclic compounds have shown that the substitution of a C=C double bond with a S atom has little effect on the energies of the first ionization potentials. Our present investigations confirm that this is also the case for ADT. As seen from Figure 4, the positions of at least the first six orbital levels in ADT and pentacene nearly coincide. In BDT, however, the effect of replacing a C=C bond with S is somewhat larger; the energy $\Delta E_{H/H-1}$ of the HOMO–HOMO−1 gap, for instance, is 0.4 eV smaller in BDT than in anthracene. Nevertheless, the photoelectron spectra of both isomers overall resemble that of anthracene (see Figure 3).

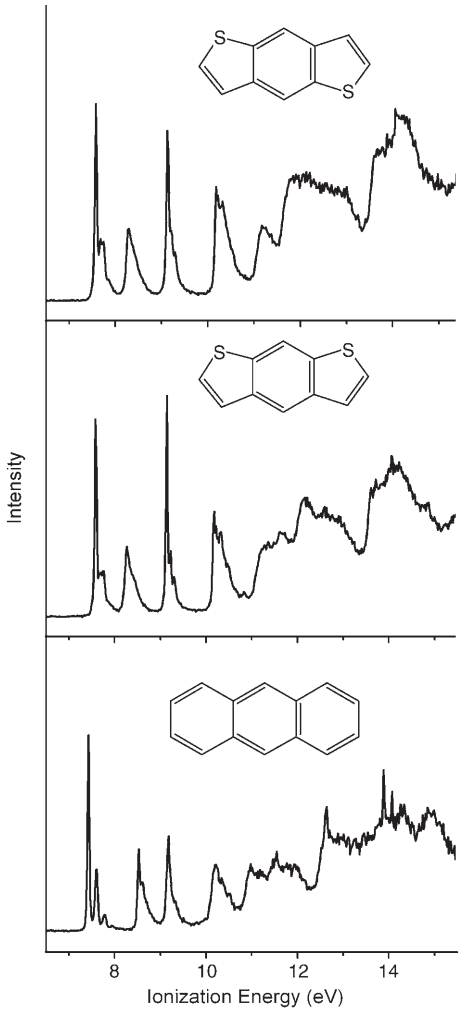

Figure 3. Gas-phase photoelectron spectra of the BDT isomers and anthracene.

Inspection of Figure 4 might suggest at first sight that the situation is completely different in TBBT. Indeed, as mentioned above, the first ionization potential in TBBT is shifted by 0.8 eV to higher energies with respect to pentacene and ADT. The calculated $\Delta E_{H/H-1}$ values (the experimental estimates of these energies is not feasible, due to the overlap of the vibrational manifolds of the ground and excited states) of 0.075 eV and 0.29 eV in *anti* and *syn* isomers, respectively, are also very different from the corresponding value (1.28 eV, DFT and 1.31 eV, experimental) obtained in pentacene. However, in view of understanding the impact of C=C to S substitution, TBBT should be rather compared with pentaphene (**9**) than with pentacene or ADT. The 7.27 eV first ionization in pentaphene[32] in fact matches very well the corresponding values of 7.36 and 7.43 eV derived for the TBBT isomers. In addition, the $\Delta E_{H/H-1}$ value of 0.12 eV estimated for pentaphene is also in good agree-

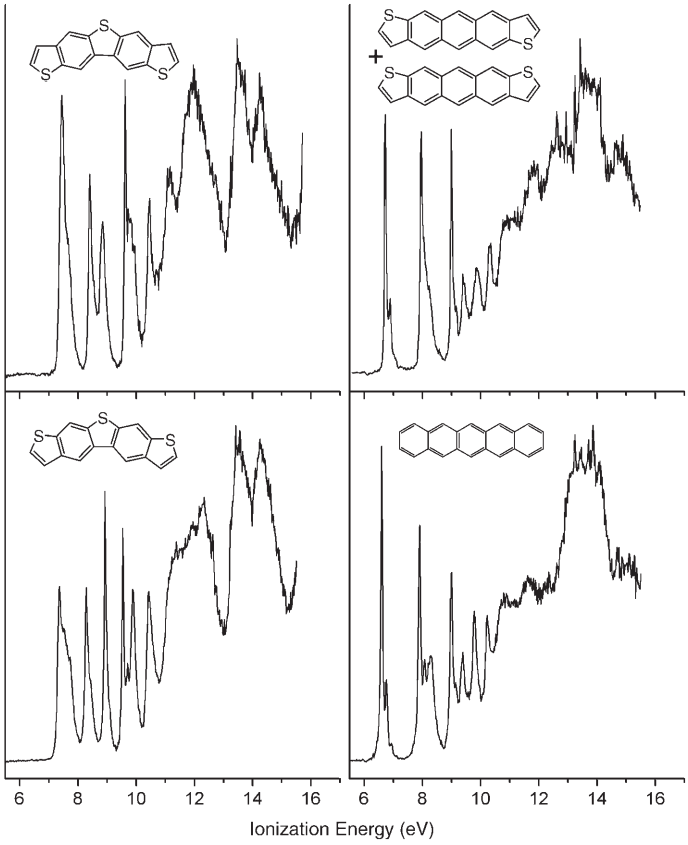

Figure 4. Gas-phase photoelectron spectra of the TBBT isomers, ADT, and pentacene.

ment with the corresponding energy gaps in TBBT isomers. The DFT calculations indicate that heterocycles **10**–**12** share the same kind of similarity with pentaphene.

Geometry: The DFT electronic-structure calculations indicate that, for all acenedithiophenes (**1**–**6**) considered here, the *anti* and *syn* isomers are nearly isoenergetic. The *anti* isomer is only slightly more stable than the *syn* isomer by 8.3 (0.19), 2 (0.045), 0.7 meV (0.016 kcal mol^{-1}) for BDT, NDT, and ADT, respectively; thus, the larger the size of the central acene segment, the smaller the energy difference between the acenedithiophene isomers. This energy difference quickly becomes insignificant.

The degree of geometry relaxations calculated when going from the neutral to the cation or anion states in BDT, NDT, and ADT is similar to those observed in the corresponding oligoacenes. BDT shows the largest geometry relaxations upon oxidation (reduction), with changes in C–C bond lengths of about 0.015(0.020) Å. This value decreases to 0.011(0.015) and 0.009(0.011) Å in NDT and ADT, respectively, pointing to a larger geometry relaxation in the anion than in the cation. The change in the C–S bond lengths for BDT is nearly the same for both oxidation (0.020 Å) and reduction (0.021 Å) processes. In contrast, the C–S bond changes upon oxidation in NDT and ADT (0.021 Å and 0.018 Å, respectively) are much larger than those upon reduction (0.008 and 0.004 Å, respectively). This can be understood from the analysis of the shape of the acenedithiophene frontier orbitals (see Supporting Information); the HOMO level presents an antibonding character between the carbon and sulfur atoms, which leads to a shortening of the C–S bonds in all acenedithiophenes when one electron is removed; in contrast, the sulfur atoms do not contribute to the LUMO level for NDT and ADT. The *syn* and *anti* isomers of TBBT present C–C bond length modifications of 0.012 and 0.005 Å upon oxidation, and 0.010 and 0.016 Å upon reduction. The change in C–S bond lengths in the terminal thiophene units (*syn*, 0.011 Å; *anti*, 0.013 Å) is smaller than that in the central thiophene unit (*syn*, 0.029 Å; *anti*, 0.030 Å) in both isomers.

Reorganization energy: Table 1 collects the DFT estimates of the reorganization energies λ associated with hole–vibrational (λ(HT)) and electron–vibrational (λ(ET)) couplings

Table 1. B3LYP/6-31G** estimates of the reorganization energies λ [eV] related to electron transfer (ET) and hole transfer (HT) in acenedithiophenes and oligoacenes.

Molecule	λ (ET)	λ (HT)
anthracene	0.200	0.137
anti-BDT	0.299	0.165
syn-BDT	0.256	0.107
tetracene	0.160	0.113
anti-NDT	0.212	0.105
syn-NDT	0.196	0.100
pentacene	0.132	0.097
anti-ADT	0.161	0.096
syn-ADT	0.159	0.094

(i.e., with hole- and electron-transfer processes) in acenedithiophenes along with those in oligoacenes. As in the case of oligoacenes, λ(ET) in acenedithiophenes is much larger than λ(HT). Also, the DFT calculations predict larger values for λ(ET) in acenedithiophenes than in their parent oligoacenes; except for *anti*-BDT, the λ(EH) values show an opposite trend. With regard to isomers, both λ(ET) and λ(HT) are larger for *anti* isomers; the differences between the isomers, however, rapidly decrease as the size of the molecules increases.

We also evaluated the partition of the reorganization energies into the contributions of each normal mode according to Equations (4) and (5). The derived vibrational couplings (Huang–Rhys factors, S_i) related to hole transfer in BDT isomers are given in Tables 2 and 3 (see Supporting Information for the electron–vibrational couplings and the corresponding data for the other systems). The reorganization energies obtained from the adiabatic potential (AP) surface calculations and the normal mode (NM) approach are in excellent agreement. While the main contribution to the reorganization energy λ(HT) in oligoacenes comes from high-energy vibrations in the range 1200–1600 cm^{-1}, this range extends from 600 to 1600 cm^{-1} in acenedithiophenes. For example, in BDT the contributions of the high energy modes

Table 2. B3LYP/6-31G** estimates of frequencies (ω), Huang–Rhys factors (S), and relaxation energies (λ_{rel}), related to hole transfer in *anti*-BDT.

Neutral			Cation		
ω [cm^{-1}]	S	λ_{rel} [eV]	ω [cm^{-1}]	S	λ_{rel} [eV]
422	0.019	0.001	411	0.039	0.002
556	0.015	0.001	540	0.015	0.001
685	0.118	0.010	682	0.059	0.005
755	0.064	0.006	763	0.074	0.007
826	0.059	0.006	851	0.104	0.011
973	0.008	0.001	974	0.025	0.003
1115	0.022	0.003	1111	0.036	0.005
1246	0.052	0.008	1241	0.032	0.005
1272	0.006	0.001	1286	0.025	0.004
1364	0.000	0.000	1396	0.012	0.002
1519	0.037	0.007	1413	0.057	0.010
1598	0.172	0.034	1555	0.062	0.012
1647	0.054	0.011	1578	0.061	0.012
total		0.089	total		0.079

Table 3. B3LYP/6-31G** estimates of frequencies (ω), Huang–Rhys factors (S), and relaxation energies (λ_{rel}), related to hole transfer in *syn*-BDT.

Neutral			Cation		
ω [cm^{-1}]	S	λ_{rel} [eV]	ω [cm^{-1}]	S	λ_{rel} [eV]
235	0.034	0.001	236	0.034	0.001
379	0.021	0.001	378	0.021	0.001
581	0.042	0.003	593	0.041	0.003
685	0.024	0.002	682	0.012	0.001
778	0.073	0.007	794	0.071	0.007
845	0.019	0.002	863	0.047	0.005
1091	0.030	0.004	1095	0.037	0.005
1258	0.032	0.005	1263	0.032	0.005
1339	0.006	0.001	1332	0.006	0.001
1459	0.006	0.001	1426	0.017	0.003
1532	0.000	0.000	1490	0.016	0.003
1607	0.136	0.027	1570	0.092	0.018
total		0.054	total		0.053

over 1200 cm^{-1} account for only 57% of the relaxation energy, to be compared with 100% in anthracene.

As found previously for ADT,[17] the C–C stretching modes around 1600 cm^{-1} yield the largest contribution to the reorganization energy λ(ET) related to electron transfer in both BDT and NDT; however, as in the case of oligoacenes,[17,18] there is a strong coupling with low-energy vibrations in the 250–400 cm^{-1} range. The electron– and hole–vibrational constants (Huang–Rhys factor) of BDT, NDT, and ADT are shown in Figure 5. As the size of the systems increases, when going from BDT to ADT, the Huang–Rhys factors for high-frequency vibrations decrease as expected. In contrast, the vibronic interaction with low-energy vibrational modes shows an opposite trend for both electrons and holes. As seen from Figure 5, the electron–vibrational interaction with low-energy vibrations is much larger than the hole–vibrational interaction; a similar pattern is also characteristic for oligoacenes.

The results of the normal-mode analysis have been further exploited to simulate the shape of the first ionization peak of the photoelectron spectrum in BDT. It is important

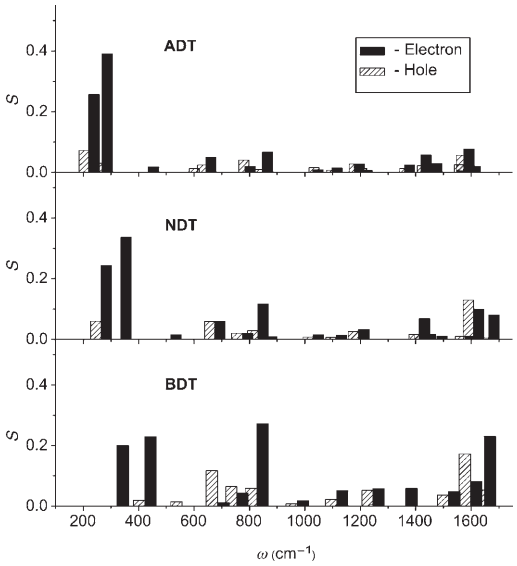

Figure 5. Huang–Rhys factors related to the electron and hole transfer, derived from the B3LYP/6-31G** calculations of the relaxation energy, $\lambda_r^{(A1)}$.

to note that the line shape of this band is directly related to the geometry relaxation energy ($\lambda_r^{(D2)}$) calculated when going from the neutral ground-state geometry to the cation optimal geometry. As seen from Tables 2 and 3, the two components $\lambda_r^{(D2)}$ and $\lambda_r^{(A1)}$ of the total reorganization energy λ(HT) [see Eq. (3)] are nearly identical; therefore, $\lambda_r^{(D2)}$ closely corresponds to half the intramolecular reorganization energy for hole transfer. The results of the simulation performed in the framework of the Born–Oppenheimer and Franck–Condon (FC) approximations (see reference [18] for more details) are shown in Figure 6. The positions of the peaks and the difference between the isomers are remarkably well reproduced. The overall agreement between the simulated and experimental spectra increases the confidence in the reliability of DFT-derived vibronic constants and relaxation energies.

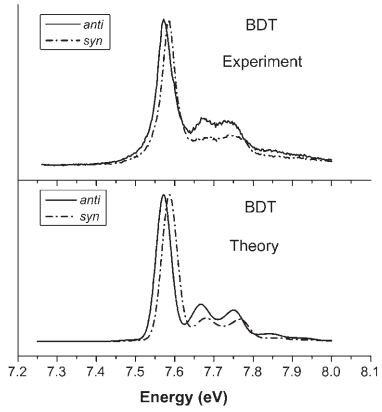

Figure 6. High-resolution close-up and B3LYP/6-31G** simulation of the vibrational structure of the first ionization of BDT isomers.

The DFT estimates of the reorganization energies λ obtained from AP calculations for the TBBT isomers and related systems are collected in Table 4. As in the case of acenedithiophenes, λ(ET) is much larger than λ(HT). The

Table 4. B3LYP/6-31G** estimates of the reorganization energies λ [eV] related to electron transfer (ET) and hole transfer (HT) in pentaphene derivatives.

Molecule	λ (ET)	λ (HT)
7	0.237	0.118
8	0.213	0.148
9	0.249	0.178
10	0.239	0.181
11	0.259	0.204
12	0.198	0.119

replacement of a C=C bond with a S atom in the terminal rings of pentaphene has only moderate influence on the relaxation energies. In contrast, replacement in the central ring results in a significant reduction of both λ(ET) and λ(HT): these two quantities in compound **12** are about 25% and 50%, respectively, smaller than in pentaphene. Both λ(ET) and λ(HT) in TBBT are also smaller than in pentaphene, while larger than in ADT and pentacene.

As already discussed above in connection with the electronic structure, the influence of the isomer constitution on the reorganization processes is more significant in TBBT than in ADT. It appears, however, that the substitution of different C=C bonds affect λ(ET) and λ(HT) in different ways. For instance, λ(ET) in *anti*-TBBT is similar to that in **10**, and is thus not affected by substitution in the middle ring. At the same time, λ(HT) in *anti*-TBBT is identical to that in **12**, indicating that the substitution in the terminal rings has no influence on the reorganization, as is further supported by the comparison of λ(HT) values in **9** and **10**.

The total reorganization energies of both TBBT isomers obtained from NM calculations (see Supporting Information) are again in excellent agreement with the corresponding values derived from AP calculations. The hole– and electron–vibrational constants are shown in Figure 7. The relaxation energy related to electron–vibrational interaction is dominated by high-energy modes with the contributions of the modes higher than 1200 cm^{-1} accounting for more than 70% of λ(ET). In contrast, hole–vibrational interactions are dominated by lower frequency modes. As seen from Figure 7, the hole–vibrational couplings (Huang–Rhys factors) for low-energy vibrational modes are significantly larger than the values derived for high-energy vibrations. The vibrational modes (at 111 and 105 cm^{-1} in *syn* and *anti* isomers, respectively) that yield the largest Huang–Rhys factors are shown in Figure 8. As a result of the better match between the orientations of the bonding/antibonding pattern of the HOMO levels and the normal-mode vector, the hole–vibrational coupling with these modes is much larger than the respective electron–vibrational coupling. As is clear from the comparison of Figures 5 and 7, the results obtained for TBBT are in marked contrast with the pattern found for

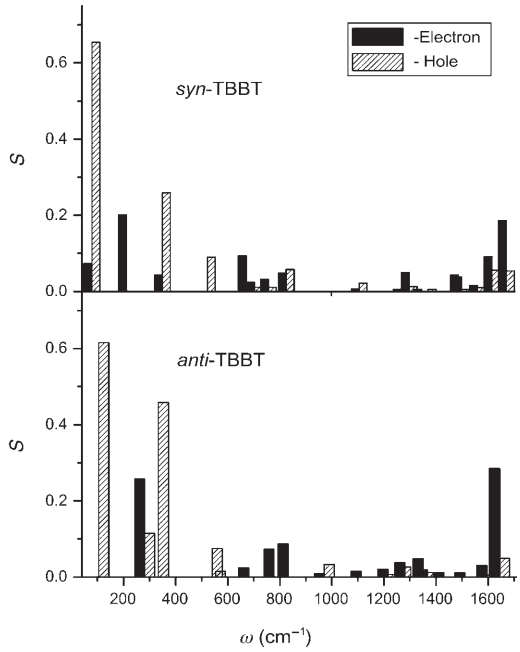

Figure 7. Electron– and hole–vibrational couplings in TBBT isomers derived from the B3LYP/6-31G** calculations of $\lambda_r^{(A1)}$.

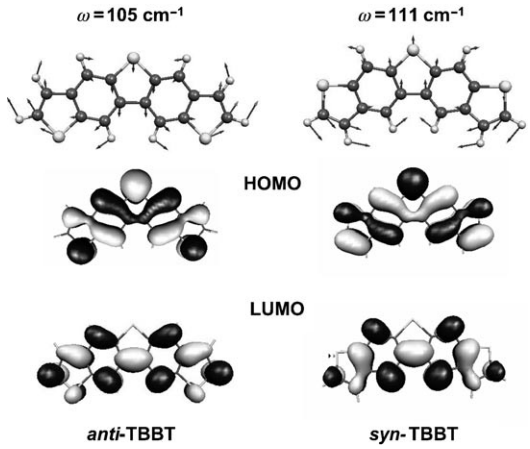

Figure 8. Illustration of the bonding/antibonding pattern of the HOMO and LUMO orbitals of TBBT isomers and the atomic displacements associated with the vibrational modes yielding the largest Huang–Rhys factors.

acenedithiophenes and oligoacenes,[18,20] in which the low-frequency modes contribute substantially only to the electron–vibrational coupling. An increase in the hole–vibrational interaction has been recently predicted as well for phenanthrene;[33] this is clearly in line with the similarity between TBBT and pentaphene discussed here.

Conclusion

We have investigated both hole–vibrational and electron–vibrational couplings in the fused thiophene–benzene compounds BDT, NDT, and TBBT. A normal-mode analysis re-

veals that the reorganization energy in acenedithiophenes, as in oligoacenes, is dominated by the interaction with high-energy vibrations, with the largest contribution coming from C–C stretching modes around 1600 cm^{-1}. However, in contrast to oligoacenes, more modes in acenedithiophenes contribute to the relaxation processes; these modes are also distributed over a larger energy range than in oligoacenes. As a consequence, as we have shown for BDT and ADT, the vibrational structure of the first ionization is not as well resolved as in the parent oligoacene systems. The DFT calculations indicate that the reorganization energies λ(ET) related to electron transfer are larger than the reorganization energies λ(HT) for hole transfer. We found a significant dependence of the relaxation processes on the isomer structure, with λ(ET) and λ(HT) being larger for the *anti* isomers. The difference between the energies of two isomers, however, is very small and keeps decreasing as the molecular size increases.

The photoelectron measurements and DFT calculations show that the electronic structure of the radical-cation state of the TBBT isomers is very different from that in ADT and pentacene, while it closely resembles the corresponding electronic structure in pentaphene. This finding is in line with previous studies of thiophene-containing heterocyclic compounds that pointed out that the substitution of a C=C double bond with a S atom has little effect on the energies of the first ionization potentials. Indeed, from the standpoint of C=C to S substitution, TBBT is a structural analogue of pentaphene rather than of pentacene or ADT. Our calculations also show that the nature of the hole–vibrational interactions in TBBT is very different from that found in acenedithiophenes, oligoacenes, and their derivatives, because of a significant coupling in TBBT between holes and low-energy vibrational modes. As a result, one can expect a much larger impact of temperature on the hole mobility in TBBT than in acenedithiophenes and oligoacenes. We also note that in TBBT the first excited state of the cation is located only about 0.1–0.2 eV above the cation ground state. This quasi-degeneracy can have a significant effect on electronic couplings and lead to an additional vibronic channel of interaction. Band-structure calculations and the calculations of inter-state vibronic couplings are in progress, in order to understand the implication of this feature on the hole-transport properties.

Acknowledgements

The work at Georgia Tech is partly supported by the National Science Foundation, through the STC for Materials and Devices for Information Technology (DMR-0120967) and through grant CHE-0343321, and by the Office of Naval Research. At Bowling Green State University, this work was begun under support from the National Science Foundation (DMR-0091689) and completed with support from ONR (N000-14-05-1-0372). One of us (B.W.) thanks the McMaster Endowment for a Fellowship and SPIE for an Educational Fellowship. D.C.N., contribution number 559 from the Center for Photochemical Sciences.

[1] J. A. Merlo, C. R. Newman, C. P. Gerlach, T. W. Kelley, D. V. Muyres, S. E. Fritz, M. F. Toney, C. D. Frisbie, *J. Am. Chem. Soc.* **2005**, *127*, 3997–4009.
[2] J. L. Brédas, D. Beljonne, V. Coropceanu, J. Cornil, *Chem. Rev.* **2004**, *104*, 4971–5003.
[3] M. Bendikov, F. Wudl, D. F. Perepichka, *Chem. Rev.* **2004**, *104*, 4891–4945.
[4] H. E. Katz, Z. N. Bao, S. L. Gilat, *Acc. Chem. Res.* **2001**, *34*, 359–369.
[5] M. M. Payne, S. R. Parkin, J. E. Anthony, *J. Am. Chem. Soc.* **2005**, *127*, 8028–8029.
[6] M. M. Payne, S. R. Parkin, J. E. Anthony, C.-C. Kuo, T. N. Jackson, *J. Am. Chem. Soc.* **2005**, *127*, 4986–4987.
[7] O. D. Jurchescu, J. Baas, T. T. M. Palstra, *Appl. Phys. Lett.* **2004**, 84, 3061–3063.
[8] J. E. Anthony, J. S. Brooks, D. L. Eaton, S. R. Parkin, *J. Am. Chem. Soc.* **2001**, *123*, 9482–9483.
[9] J. E. Anthony, D. L. Eaton, S. R. Parkin, *Org. Lett.* **2002**, *4*, 15–18.
[10] H. Meng, M. Bendikov, G. Mitchell, R. Helgeson, F. Wudl, Z. Bao, T. Siegrist, C. Kloc, C. H. Chen, *Adv. Mater.* **2003**, *15*, 1090–1093.
[11] H. E. Katz, Z. Bao, *J. Phys. Chem. B* **2000**, *104*, 671–678.
[12] J. G. Laquindanum, H. E. Katz, A. J. Lovinger, *J. Am. Chem. Soc.* **1998**, *120*, 664–672.
[13] B. Wex, B. R. Kaafarani, D. C. Neckers, *J. Org. Chem.* **2004**, *69*, 2197–2199, and references therein.
[14] B. Wex, B. R. Kaafarani, K. Kirschbaum, D. C. Neckers, *J. Org. Chem.* **2005**, *70*, 4502–4505.
[15] B. Wex, B. R. Kaafarani, A. G. Oliver, J. A. K. Bauer, D. C. Neckers, *J. Org. Chem.* **2003**, *68*, 8258–8260.
[16] M. M. Payne, S. A. Odom, S. R. Parkin, J. E. Anthony, *Org. Lett.* **2004**, *6*, 3325–3328.
[17] O. Kwon, V. Coropceanu, N. E. Gruhn, J. C. Durivage, J. G. Laquindanum, H. E. Katz, J. Cornil, J. L. Brédas, *J. Chem. Phys.* **2004**, *120*, 8186–8194.
[18] M. Malagoli, V. Coropceanu, D. A. da Silva, J. L. Brédas, *J. Chem. Phys.* **2004**, *120*, 7490–7496.
[19] D. A. da Silva, R. Friedlein, V. Coropceanu, G. Ohrwall, W. Osikowicz, C. Suess, S. L. Sorensen, S. Svensson, W. R. Salaneck, J. L. Brédas, *Chem. Commun.* **2004**, 1702–1703.
[20] V. Coropceanu, M. Malagoli, D. A. da Silva, N. E. Gruhn, T. G. Bill, J. L. Brédas, *Phys. Rev. Lett.* **2002**, *89*, 275503.
[21] N. E. Gruhn, D. A. da Silva, T. G. Bill, M. Malagoli, V. Coropceanu, A. Kahn, J. L. Brédas, *J. Am. Chem. Soc.* **2002**, *124*, 7918–7919.
[22] J. Cornil, N. E. Gruhn, D. A. dos Santos, M. Malagoli, P. A. Lee, S. Barlow, S. Thayumanavan, S. R. Marder, N. R. Armstrong, J. L. Brédas, *J. Phys. Chem. A* **2001**, *105*, 5206–5211.
[23] M. Pope, C. E. Swenberg, M. Pope, *Electronic Processes in Organic Crystals and Polymers*, 2nd ed., Oxford University Press: New York, **1999**, p. 1328.
[24] E. A. Silinsh, V. Capek, *Organic Molecular Crystals: Interaction, Localization, and Transport Phenomena*, American Institute of Physics, New York, **1994**, p. 402.
[25] Y. A. Berlin, G. R. Hutchison, P. Rempala, M. A. Ratner, J. Michl, *J. Phys. Chem. A* **2003**, *107*, 3970–3980.
[26] P. F. Barbara, T. J. Meyer, M. A. Ratner, *J. Phys. Chem.* **1996**, *100*, 13148–13168.
[27] K. D. Demadis, C. M. Hartshorn, T. J. Meyer, *Chem. Rev.* **2001**, *101*, 2655–2685.
[28] G. R. Hutchison, M. A. Ratner, T. J. Marks, *J. Am. Chem. Soc.* **2005**, *127*, 2339–2350.
[29] Gaussian 98 (Revision A.11), M. J. Frisch, G. W. Trucks, H. B. Schlegel, G. E. Scuseria, M. A. Robb, J. R. Cheeseman, V. G. Zakrzewski, J. A. Montgomery, Jr., R. E. Stratmann, J. C. Burant, S. Dapprich, J. M. Millam, A. D. Daniels, K. N. Kudin, M. C. Strain, O. Farkas, J. Tomasi, V. Barone, M. Cossi, R. Cammi, B. Mennucci, C. Pomelli, C. Adamo, S. Clifford, J. Ochterski, G. A. Petersson, P. Y. Ayala, Q. Cui, K. Morokuma, P. Salvador, J. J. Dannenberg, D. K. Malick, A. D. Rabuck, K. Raghavachari, J. B. Foresman, J. Cioslowski, J. V.

Ortiz, A. G. Baboul, B. B. Stefanov, G. Liu, A. Liashenko, P. Piskorz, I. Komaromi, R. Gomperts, R. L. Martin, D. J. Fox, T. Keith, M. A. Al-Laham, C. Y. Peng, A. Nanayakkara, M. Challacombe, P. M. W. Gill, B. Johnson, W. Chen, M. W. Wong, J. L. Andres, C. Gonzalez, M. Head-Gordon, E. S. Replogle, J. A. Pople, Gaussian, Inc., Pittsburgh PA, **2001**.

[30] R. A. W. Johnston, F. A. Mellon, *J. Chem. Soc. Faraday Trans. 2* **1973**, *69*, 1155–1163.

[31] P. Rademacher, B. Kettler, K. Kowski, M. E. Weiss, *Spectrochim. Acta Part A* **2001**, 57, 2475–2483.

[32] W. Schmidt, *J. Chem. Phys.* **1977**, *66*, 828–845.

[33] T. Kato, T. Yamabe, *J. Chem. Phys.* **2004**, *120*, 3311–3322.

Received: July 25, 2005
Published online: January 10, 2006

